



Notched graphite under multiaxial loading

S.M.J. Razavi, M. Peron, J. Torgersen, F. Berto

Department of Mechanical and Industrial Engineering, Norwegian University of Science and Technology (NTNU), Norway
javad.razavi@ntnu.no, mirco.peron@ntnu.no, jan.torgersen@ntnu.no, filippo.berto@ntnu.no

ABSTRACT. Cylindrical specimens made of polycrystalline graphite and weakened by circumferential V-notches under mixed mode I/III loading were studied in this research. Different geometries of V-notches varying the notch opening angle and the notch tip radius were tested. Applying various ratios of tensile and torsion loads, the multiaxial static tests have been conducted. Averaged Strain Energy Density (ASED) criterion previously presented by the same authors is employed here for the case of tension and torsion loadings applied in combination. The fracture behavior of the tested joints under multiaxial loading has been successfully predicted using the ASED criterion.

KEYWORDS. Isostatic polycrystalline graphite; Mixed mode I/III; V-notch; Strain energy density.



Citation: Razavi, S.M.J., Peron, M., Torgersen, J., Berto, F., Notched graphite under multiaxial loading, *Frattura ed Integrità Strutturale*, 41 (2017) 424-431.

Received: 15.05.2017

Accepted: 23.05.2017

Published: 01.07.2017

Copyright: © 2017 This is an open access article under the terms of the CC-BY 4.0, which permits unrestricted use, distribution, and reproduction in any medium, provided the original author and source are credited.

INTRODUCTION

Due to its good compromise between thermal and mechanical properties, isostatic graphite is widely used in various industrial applications. A bulk number of the components made of graphite is subjected to loads transferred by the other parts of the structure. According to this fact, numerous researches have been devoted to the fracture assessment of graphite. Considering the brittle behavior of this material, brittle fracture is a typical failure mechanism which usually happens after the initiation of micro-cracks in the most stressed parts of the structure, combined in some cases with a negligible amount of plasticity [1-4]. The majority of the studies focused on structural integrity of graphite components have been devoted to the investigation of cracked components by quantifying the fracture toughness under prevalent mode I loading [5-7]. Innovative techniques have been proposed in the literature for fracture assessment of isotropic graphite under mode I loading [8-10]. Although the brittle fracture of graphite components has been studied continuously for several years, only few predictive models are available for the fracture behavior of cracked components.

Reviewing the published papers in the field of fracture behavior of graphite components reveals that only a limited number of researches are focused on the notch sensitivity of graphite components including the researches conducted by Bazaj and Cox [8] and Kawakami [9]. The fracture behavior of blunt notches has been studied in the past years by researchers, who have investigated the case of pure mode I loading and in-plane mixed mode loading [11-18].

Due to the lack of information about the multiaxial behavior of graphite components in the literature, the authors aimed to investigate the static behavior of isostatic graphite subjected to multiaxial loadings which can be applied as a

combination of tension and torsion with different values of the mode mixity ratios (i.e. the ratio between the tensile stress and the applied stress due to torsion loading): 0.4, 0.5 and 1.0. Considering a large variety of geometrical configurations obtained by varying the notch opening angle, notch radius and notch depth, a complete set of experimental data on cylindrical specimens subjected to combined tension and torsion loads was provided by the authors in previous paper [23]. The notch opening angle has been varied from 30° to 120° and the notch radius from 0.3 to 2 mm.

The ASED criterion which is based on the strain energy density averaged over a control volume [19-25] is used for fracture assessment of notched samples subjected to the multiaxial static loading. The ASED criterion allows a sound fracture assessment of the critical load for the specific material under investigation and it can be potentially extended to other types of graphite and brittle materials subjected to different combinations of mode I and mode III loading conditions. In the current paper, first the experimental procedure for testing the notched graphite samples is presented. Afterward, the formulation and application of the ASED criterion is presented on the experimental data.

FRACTURE EXPERIMENTS

The details of the graphite material, the test specimens and the fracture experiments are presented in this section. The fracture tests were conducted on a grade of isostatic polycrystalline graphite with commercial name of EG022A. The basic material properties of the tested graphite are as follows: the mean grain size is of $300\ \mu\text{m}$, the porosity of 15%, the bulk density of $1830\ \text{kg}/\text{m}^3$, the mean tensile strength of 30 MPa, the Young's modulus of 8.00 GPa and the shear modulus of 3.30 GPa. Nonlinear deformation sometimes is observed during fracture tests of graphites, which makes the determination of Young's modulus rather complicated. However, for simplicity the Young's modulus was obtained in this research from load-displacement graphs recorded by a universal tension-compression machine. The deviation observed from linear behaviour was less than 0.01% at failure for the specimen used in the test. Young's modulus has been measured at a load where the deviation from linear behaviour was less than 0.005%. The mean grain size was given in the material certify and measured by using the SEM technique while the density of the material was determined from the buoyancy method, submerging the tested graphite in a liquid of known density. The values have been checked and confirmed by the authors independently.

All tests were performed under displacement control on a servo-controlled MTS bi-axial testing device ($\pm 100\ \text{kN}/\pm 1100\ \text{Nm}$, $\pm 75\ \text{mm}/\pm 55^\circ$). The load was measured by a MTS cell with $\pm 0.5\ \%$ error at full scale. A MTS strain gauge axial extensometer (MTS 632.85F-14), with a gage length equal to 25 mm was used for measuring the tensile elastic properties on plain specimens while a multi-axis extensometer MTS 632.80F-04 (with a gage length equal to 25 mm) was used for measuring the torsional elastic properties on unnotched specimens.

Some load-displacement curves were recorded to obtain the Young's modulus (E) of the graphite using an axial extensometer. The tensile strength (σ_t) was measured by means of axis-symmetric specimens with a net diameter equal to 12.5 mm and a diameter of 20 mm on the gross section (see Fig. 1a). Due to the presence of a root radius equal to 40 mm, the theoretical stress concentration factor is less than 1.03.

The torque-angle graphs recorded by the MTS device were employed together with the bi-axis extensometer to obtain the shear modulus (G) and to measure the torsion strength (τ_t) of the tested graphite. The ultimate shear strength τ_t was found to be equal to 37 MPa.

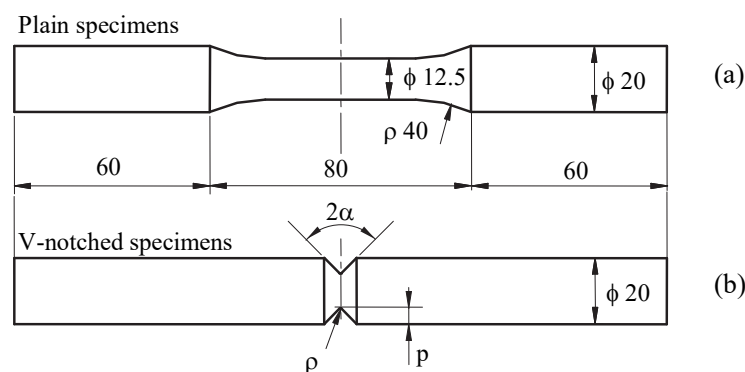


Figure 1: Geometry of plain (a) and notched (b) specimens used in the experimental tests.



As shown in Fig. 1, different round bar specimens were used for multiaxial (tension and torsion) static tests: unnotched specimens (Fig. 1a) and cylindrical specimens with V-notches (Fig. 1b). This allows us to explore the influence of a large variety of notch shapes in the experiments.

In more detail:

- For V-notched graphite specimens with a notch opening angle $2a = 120^\circ$ (Fig. 1b), notches with four different notch root radii were tested; $\rho = 0.3, 0.5, 1$ and 2.0 mm. The effect of net section area was studied by changing the notch depth p . Two values were used, $p = 3$ and 5 mm, while keeping the gross diameter constant (20 mm).
- For V-notched graphite specimens with a notch opening angle $2a = 60^\circ$ (Fig. 1b), four different notch root radii were considered in the experiments: $\rho = 0.3, 0.5, 1.0$ and 2.0 mm. With a constant gross diameter (20 mm), also the net section area was kept constant, such that $p = 5$ mm.
- For V-notched graphite specimens with a notch opening angle $2a = 30^\circ$ (Fig. 1b), three different notch root radii were considered in the experiments: $\rho = 0.5, 1.0$ and 2.0 mm keeping constant the notch depth $p = 5$ mm.

At least three samples were prepared for each of the 15 specimen geometries described above, with a total number of 45 specimens. In order to prepare the specimens, first several thick plates were cut from a graphite block. Then, the specimens were precisely manufactured by using a 2-D CNC cutting machine. Before conducting the experiments, the cut surfaces of the graphite specimens were polished by using a fine abrasive paper to remove any possible local stress concentrations due to surface roughness. The tests were conducted under three different combinations of tensile and torsional stresses, with the nominal mode mixity ratios $\sigma_{nom}/\tau_{nom} = 0.4, 0.5$ and 1 . Different nominal mode mixity ratios have been achieved by properly setting the torsional loading rate with respect to the tensile loading rate. In particular the tensile loading rate was varied keeping constant the rotation control conditions with a loading rate of $1^\circ/\text{min}$. The load-angle curves recorded during the tests always exhibited an approximately linear trend up to the final failure, which occurred suddenly. Therefore, the use of a fracture criterion based on a linear elastic hypothesis for the material law is realistic. The same trend has been observed for the tensile curves plotting the load as a function of the axial displacement. All loads to failure (tensile load and torque) are reported in Tabs. 1-3 for each notch configuration and loading conditions. In particular Tab. 1 reports the data for $\sigma_{nom}/\tau_{nom} = 1$ while Tabs. 2 and 3 summarize the data for the two ratios 0.4 and 0.5 , respectively.

Specimen code	Notch opening angle $2a$ ($^\circ$)	Notch radius ρ (mm)	Tensile Load (N)	Torque (N mm)	σ_{nom} (MPa)	τ_{nom} (MPa)	σ_{nom}/τ_{nom}
1-01	120°	0.3	1193	2659	15.19	13.54	1.12
1-02			1025	2280	13.05	11.61	1.12
1-03			1114	2500	14.18	12.73	1.11
2-01		0.5	1190	2690	15.15	13.69	1.10
2-02			1234	2631	15.71	13.40	1.17
2-03			1200	2694	15.28	13.72	1.11
3-01		1	1302	2873	16.58	14.63	1.13
3-02			1251	2673	15.93	13.61	1.17
3-03			1283	2845	16.34	14.49	1.13
4-01	2	1497	3798	19.06	19.35	0.98	
4-02		1451	3634	18.47	18.51	1.00	
4-03		1532	3710	19.51	18.89	1.03	
5-01	60°	0.3	1073	2632	13.66	13.40	1.02
5-02			1037	2867	13.20	14.60	0.90
5-03			1125	2883	14.32	14.68	0.98
6-01	30°	0.5	1097	2852	13.97	14.53	0.96
6-02			1157	2704	14.73	13.75	1.07
6-03			1213	2917	15.44	14.86	1.04
7-01	1	1178	3038	15.00	15.47	0.97	
7-02		1112	2972	14.16	15.14	0.94	
7-03		1214	3248	15.46	16.54	0.93	
8-01	2	1302	3102	16.55	15.80	1.05	
8-02		1319	3386	16.79	17.24	0.97	
8-03		1486	3489	18.92	17.77	1.06	

Table 1: Experimental results in the case of $\sigma_{nom}/\tau_{nom} = 1.0$; notch depth $p = 5$ mm.



Specimen code	Notch opening angle $2a$ ($^{\circ}$)	Notch radius ρ (mm)	Tensile Load (N)	Torque (N mm)	σ_{nom} (MPa)	τ_{nom} (MPa)	σ_{nom}/τ_{nom}
9-01	60	0.5	636	3923	8.10	19.98	0.41
9-02			600	4010	7.64	20.42	0.38
9-03			630	4009	8.02	20.42	0.39
10-01		1	645	4449	8.21	22.66	0.36
10-02			660	4634	8.40	23.60	0.36
10-03			631	4326	8.03	22.03	0.36
11-01		2	895	5164	11.40	26.30	0.43
11-02			811	5259	10.33	26.78	0.39
11-03			750	4700	9.55	23.94	0.40

Table 2: Experimental results in the case of $\sigma_{nom}/\tau_{nom} = 0.4$; notch depth $p = 5$ mm.

Specimen code	Notch opening angle $2a$ ($^{\circ}$)	Notch radius ρ (mm)	Tensile Load (N)	Torque (N mm)	σ_{nom} (MPa)	τ_{nom} (MPa)	σ_{nom}/τ_{nom}
12-01	120	0.3	1482	11606	9.63	21.54	0.45
12-02			1324	9657	8.60	17.92	0.48
12-03			1768	12129	11.49	22.51	0.51
13-01		0.5	1701	11768	11.05	21.84	0.51
13-02			1619	11196	10.52	20.78	0.51
13-03			1657	12005	10.76	22.28	0.48
14-01		1	1739	12150	11.30	22.55	0.50
14-02			1788	12756	11.62	23.68	0.49
14-03			1816	12611	11.80	23.41	0.50
15-01		2	2034	13891	13.21	25.78	0.51
15-02			1756	12500	11.41	23.20	0.49
15-03			1931	13452	12.54	24.97	0.50

Table 3: Experimental results in the case of $\sigma_{nom}/\tau_{nom} = 0.5$; notch depth $p = 3$ mm.

As visible from the tables the imposed mode mixity ratio is almost fulfilled with a variation of approximately $\pm 10\%$ with respect to the nominal value. The variability of the loads to failure as a function of the notch opening angle is weak although not negligible. For a constant notch radius, the fracture load slightly increases for larger notch opening angles, although this effect is very low.

STRAIN ENERGY DENSITY AVERAGED OVER A CONTROL VOLUME: THE FRACTURE CRITERION

With the aim to assess the fracture load in notched graphite components, an appropriate fracture criterion is required which has to be based on the mechanical behaviour of material around the notch tip. In this section, a criterion proposed by Lazzarin and co-authors [19] based on the strain energy density (SED) is briefly described. The averaged strain energy density criterion (SED) states that brittle failure occurs when the mean value of the strain energy density over a given control volume is equal to a critical value W_c . This critical value varies from material to material but it does not depend on the notch geometry and sharpness. The control volume is considered to be dependent on the ultimate tensile strength σ_t and the fracture toughness K_{Ic} in the case of brittle or quasi-brittle materials subjected to static tensile loads.

The method based on the averaged SED was formalised and applied first to sharp (zero radius) V-notches under mode I and mixed mode I+II loading [19] and later extended to blunt U- and V-notches [20]. When dealing with cracks, the control volume is a circle of radius R_c centred at the crack tip (Fig. 2a). Under plane strain conditions, the radius R_c can be evaluated according to the following expression [26]:

$$R_{Ic} = \frac{(1+\nu)(5-8\nu)}{4\pi} \left(\frac{K_{Ic}}{\sigma_t} \right)^2 \quad (1)$$

where K_{Ic} is the mode I fracture toughness, ν the Poisson's ratio and σ_t the ultimate tensile stress of a plain specimen. For a sharp V-notch, the critical volume becomes a circular sector of radius R_c centred at the notch tip (Fig. 2b). When only failure data from open V-notches are available, R_c can be determined on the basis of some relationships where K_{Ic} is substituted by the critical value of the notch stress intensity factors (NSIFs) as determined at failure from sharp V-notches. Dealing here with sharp notches under torsion loading, the control radius R_{3c} can be estimated by means of the following equation:

$$R_{3c} = \left(\sqrt{\frac{e_3}{1+\nu}} \frac{K_{3c}}{\tau_t} \right)^{\frac{1}{1-\lambda_3}} \quad (2)$$

where K_{3c} is the mode III critical notch stress intensity factor and τ_t is the ultimate torsion strength of the unnotched material. Moreover, e_3 is the parameter that quantifies the influence of all stresses and strains over the control volume and $(1-\lambda_3)$ is the degree of singularity of the linear elastic stress fields [27], which depends on the notch opening angle. Values of e_3 and λ_3 are 0.4138 and 0.5 for the crack case ($2\alpha = 0^\circ$).

For a blunt V-notch under mode I or mode III loading, the volume is assumed to be of a crescent shape (as shown in Fig. 2c), where R_c is the depth measured along the notch bisector line. The outer radius of the crescent shape is equal to $R_c + r_0$, being r_0 the distance between the notch tip and the origin of the local coordinate system (Fig. 2c). Such a distance depends on the V-notch opening angle 2α , according to the expression:

$$r_0 = \rho \frac{(\pi - 2\alpha)}{(2\pi - 2\alpha)} \quad (3)$$

For the sake of simplicity, complex theoretical derivations have deliberately been avoided in the present work and the SED values have been determined directly from the FE models.

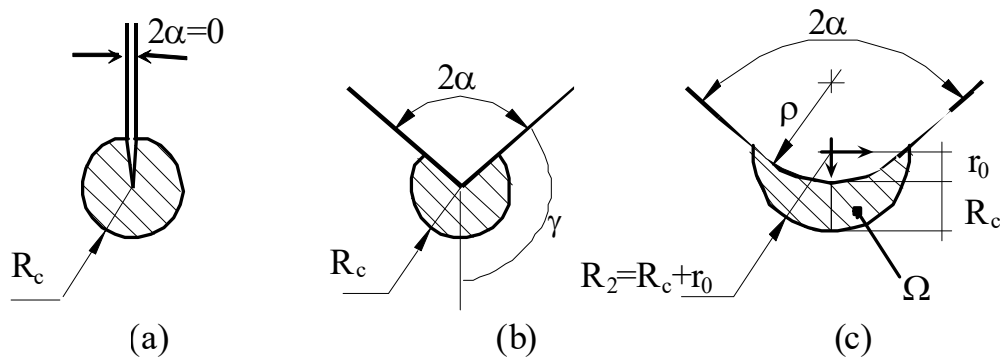


Figure 2: Control volume for (a) crack, (b) sharp V-notch and (c) blunt V-notch, under mixed mode I+III loading.

SED APPROACH IN FRACTURE ANALYSIS OF THE TESTED GRAPHITE SPECIMENS

The fracture criterion described in the previous section is employed here to estimate the fracture loads obtained from the experiments conducted on the graphite specimens. In order to determine the SED values, first a finite element model of each graphite specimen was generated. As originally thought for pure modes of loading the averaged strain energy density criterion (SED) states that failure occurs when the mean value of the strain energy density over a control volume, \bar{W} , reaches a critical value W_c , which depends on the material but not on the notch geometry. Under tension loads, this critical value can be determined from the ultimate tensile strength σ_t according to Beltrami's expression for the unnotched material:

$$W_{Ic} = \frac{\sigma_t^2}{2E} \quad (4)$$



By using the values of $\sigma_t = 30$ MPa and $E = 8000$ MPa, the critical SED for the tested graphite is $W_{1c} = 0.05625$ MJ/m³. Under torsion loads, this critical value can be determined from the ultimate shear strength τ_t according to Beltrami's expression for the unnotched material:

$$W_{3c} = \frac{\tau_t^2}{2G} \tag{5}$$

By using the values of $\tau_t = 37$ MPa and $G = 3300$ MPa, the critical SED for the tested graphite is $W_{3c} = 0.2074$ MJ/m³. In parallel, the control volume definition via the control radius R_c needs the knowledge of the mode I and mode III critical notch stress intensity factor K_{Ic} and K_{3c} and the Poisson's ratio ν , see Eqs (1) and (2). For the considered material K_{Ic} and K_{3c} have been obtained from specimens weakened by sharp V-notches with an opening angle $2\alpha = 10^\circ$ and a notch radius less than 0.1 mm. A pre-crack was also generated with a razor blade at the notch tip. The resulting values are $K_{Ic} = 1.06$ MPa m^{0.5} and $K_{3c} = 1.26$ MPa m^{0.5} which provide the control radii $R_{1c} = 0.405$ mm and $R_{3c} = 0.409$ mm, under pure tension and pure torsion, respectively. For the sake of simplicity, a single value of the control radius was kept for the synthesis in terms of SED setting $R_c = R_{1c} = R_{3c}$.

As discussed in previous papers [20,21], the control radii under tension and torsion can be very different and this is particularly true when the material behaviour differs from a brittle one: the difference is higher for materials obeying a ductile behaviour. For this specific case, the values are so close to each other that a single value can be employed for the final synthesis. The SED criterion has been applied here for the first time to mixed mode I+III loading conditions.

The proposed formulation is a reminiscent of the work by Gough and Pollard [28] who proposed a stress-based expression able to summarize together the results obtained from bending and torsion. The criterion was extended in terms of the local SED to V-notches under fatigue loading in the presence of combined tension and torsion loadings [29]. In agreement with Lazzarin et al. [29, 30] and by extending the method to the static case, the following elliptic expression:

$$\frac{\bar{W}_1}{W_{1c}} + \frac{\bar{W}_3}{W_{3c}} = 1 \tag{6}$$

is obtained. In Eq. (6) W_{1c} and W_{3c} are the critical values of SED under pure tension and pure torsion. For the considered graphite, $W_{1c} = 0.05625$ MJ/m³ and $W_{3c} = 0.2074$ MJ/m³. The values of \bar{W}_1 and \bar{W}_3 have, instead, to be calculated as a function of the notch geometry and of the applied mode mixity ratio. Each specimen reaches its critical energy when the sum of the weighted contributions of mode I and mode III is equal to 1, which represents the complete damage of the specimen.

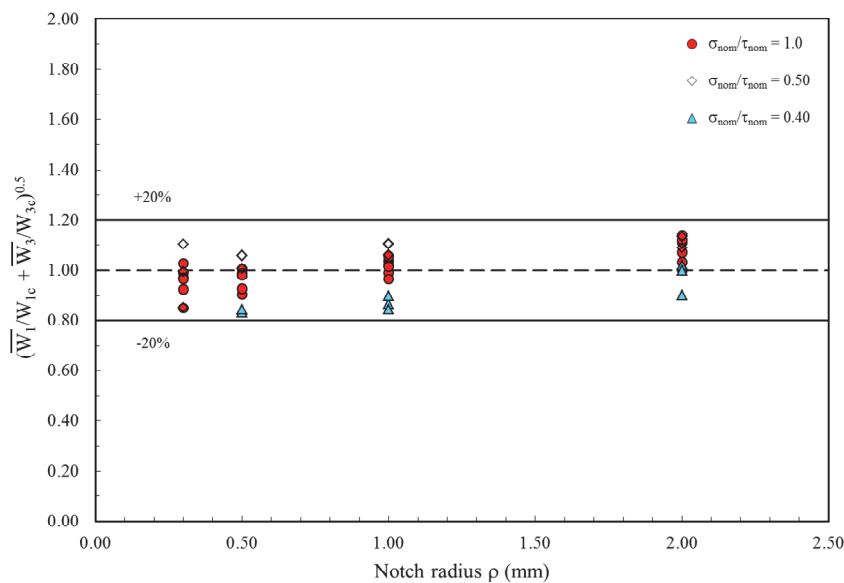


Figure 3: Synthesis of the results from combined tension and torsion tests based on the averaged SED.



A synthesis in terms of the square root value of the considered parameter, that is the sum of the weighted energy contributions related to mode I and mode III loading, is shown in Fig. 3 as a function of the notch root radius ρ . The obtained trend is very promising. Many of the results are inside a scatter band ranging from 0.9 to 1.1 with only few exceptions. The fracture model proposed in this paper can be used for predicting the onset of brittle fracture in notched graphite components which are subjected to a combination of tension and torsion loadings. Such criterion would be very useful for designers and engineers who should explore the safe performance of graphite components particularly under complex loading conditions.

CONCLUSIONS

Brittle fracture in V-notched polycrystalline graphite specimens was investigated both experimentally and theoretically under combined tension and torsion loading. Fracture tests were conducted on notched round bar graphite specimens. Different notch depths, notch radii and opening angles were considered in the test specimens as well as different combinations of the mode mixity ratio σ_{nom}/τ_{nom} . The new set of data provided in the paper is unique because no previous papers have been devoted to similar topics dealing with graphite components.

The SED criterion was used for the first time in order to estimate the fracture load of notched graphite components under mixed mode I+III static loading. A new formulation of the SED criterion was proposed showing the capabilities of the suggested method to assess the fracture behaviour of polycrystalline graphite under the considered loading conditions. The results estimated by the SED approach were found to be in good agreement with the experimental results. The criterion based on the elliptic expression described above seems to be very advantageous because it requires, as experimental parameters, only the critical energies from unnotched graphite specimens under pure tension and pure torsion.

REFERENCES

- [1] Sakai, M., Urashima, K., Inagaki, M., Energy Principle of Elastic-Plastic Fracture and Its Application to the Fracture Mechanics of a Polycrystalline Graphite, *J. Am. Ceram. Soc.*, 66 (1983) 868–874. DOI: 10.1111/j.1151-2916.1983.tb11003.x.
- [2] Ayatollahi, M.R., Razavi, S.M.J., Rashidi Moghaddam, M., Berto, F., Mode I fracture analysis of Polymethylmetacrylate using modified energy—based models, *Phys. Mesomech.*, 18(5) (2015) 53-62. DOI: 10.1134/S1029959915040050.
- [3] Ayatollahi, M.R., Rashidi Moghaddam, M., Razavi, S.M.J., Berto, F., Geometry effects on fracture trajectory of PMMA samples under pure mode-I loading, *Eng. Fract. Mech.*, 163 (2016) 449–461. DOI: 10.1016/j.engfracmech.2016.05.014.
- [4] Rashidi Moghaddam, M., Ayatollahi, M.R., Razavi, S.M.J., Berto, F., Mode II Brittle Fracture Assessment Using an Energy Based Criterion, *Phys. Mesomech.* (in press).
- [5] Hess, P., Graphene as a model system for 2D fracture behavior of perfect and defective solids, *Frattura ed Integrità Strutturale*, 9(34) (2015) 341-346. DOI: 10.3221/IGF-ESIS.34.37.
- [6] Vo, T.T.G., Martinuzzi, P., Tran, V.X., McLachlan, N., Steer, A., Modelling 3D crack propagation in ageing graphite bricks of Advanced Gas-cooled Reactor power plant, *Frattura ed Integrità Strutturale*, 9(34) (2015) 237-245. DOI: 10.3221/IGF-ESIS.34.25.
- [7] Doddamani, S., Kaleemulla, M., Experimental investigation on fracture toughness of Al6061–graphite by using circumferential notched tensile specimens, *Frattura ed Integrità Strutturale*, 11(39) (2017) 274-281. DOI: 10.3221/IGF-ESIS.39.25.
- [8] Bazaj, D.K., Cox, E.E., Stress-concentration factors and notch-sensitivity of graphite, *Carbon*, 7 (1969) 689–697. DOI: 10.1016/0008-6223(69)90524-7.
- [9] Kawakami, H., Notch sensitivity of graphite materials for VHTR, *Trans. Atomic Energy Soc. Jpn.*, 27 (1985) 357–364. DOI: 10.3327/jaesj.27.357.
- [10] Sato, S., Awaji, H., Akuzawa, H., Fracture toughness of reactor graphite at high temperature, *Carbon*, 16 (1978) 95–102. DOI: 10.1016/0008-6223(78)90004-0.
- [11] Ayatollahi, M.R., Berto, F., Lazzarin, P., Mixed mode brittle fracture of sharp and blunt V-notches in polycrystalline graphite, *Carbon*, 49 (2011) 2465–2474. DOI: 10.1016/j.carbon.2011.02.015.



- [12] Berto, F., Lazzarin, P., Ayatollahi, M.R., Brittle fracture of sharp and blunt V-notches in isostatic graphite under torsion loading, *Carbon*, 50 (2012) 1942–1952. DOI: 10.1016/j.carbon.2011.12.045.
- [13] Lazzarin, P., Berto, F., Ayatollahi, M.R., Brittle failure of inclined key-hole notches in isostatic graphite under in-plane mixed mode loading, *Fatigue Fract. Eng. Mater. Struct.*, 36 (2013) 942–955. DOI: 10.1111/ffe.12057.
- [14] Berto, F., Lazzarin, P., Ayatollahi, M.R., Brittle fracture of sharp and blunt V-notches in isostatic graphite under pure compression loading, *Carbon*, 63 (2013) 101–116. DOI: 10.1016/j.carbon.2013.06.045.
- [15] Berto, F., Lazzarin, P., Marangon, C., Brittle fracture of U-notched graphite plates under mixed mode loading, *Mater. Des.*, 41 (2012) 421–432. DOI: 10.1016/j.matdes.2012.05.022.
- [16] Radaj, D., Berto, F., Lazzarin, P., Local fatigue strength parameters for welded joints based on strain energy density with inclusion of small-size notches, *Eng. Fract. Mech.*, 76(8) (2009) 1109-1130. DOI: 10.1016/j.engfracmech.2009.01.009.
- [17] Lazzarin, P., Campagnolo, A., Berto, F., A comparison among some recent energy- and stress-based criteria for the fracture assessment of sharp V-notched components under mode I loading, *Theor. Appl. Fract. Mech.*, 71 (2014) 21-30. DOI: 10.1016/j.tafmec.2014.03.001.
- [18] Radaj, D., Lazzarin, P., Berto, F., Generalised Neuber concept of fictitious notch rounding, *Int. J. Fatigue*, 51 (2013) 105-115. DOI: 10.1016/j.ijfatigue.2013.01.005.
- [19] Lazzarin, P., Zambardi, R., A finite-volume-energy based approach to predict the static and fatigue behaviour of components with sharp V-shaped notches, *Int. J. Fract.*, 112 (2001) 275-298. DOI: 10.1023/A:1013595930617.
- [20] Lazzarin, P., Berto, F., Some expressions for the strain energy in a finite volume surrounding the root of blunt V-notches, *Int. J. Fract.*, 135 (2005) 161–185. DOI: 10.1007/s10704-005-3943-6.
- [21] Berto, F., Lazzarin, P., A review of the volume-based strain energy density approach applied to V-notches and welded structures, *Theor. Appl. Fract. Mech.*, 52 (2009) 183–194. DOI: 10.1016/j.tafmec.2009.10.001.
- [22] Berto, F., Lazzarin, P., Recent developments in brittle and quasi-brittle failure assessment of engineering materials by means of local approaches, *Mater. Sci. Eng. R Reports*, 75 (2014) 1–48. DOI: 10.1016/j.mser.2013.11.001.
- [23] Berto, F., Campagnolo, A., Ayatollahi, M.R., Brittle Fracture of Rounded V-Notches in Isostatic Graphite under Static Multiaxial Loading, *Phys. Mesomech.*, 18 (2015) 283–297. DOI: 10.1134/S1029959915040025.
- [24] Berto, F., Ayatollahi, M., Campagnolo, A., Fracture tests under mixed mode I + III loading: an assessment based on the local energy, *Int. J. Damage Mech.*, (in press). DOI: 10.1177/1056789516628318.
- [25] Campagnolo, A., Berto, F., Leguillon, D., Fracture assessment of sharp V-notched components under Mode II loading: a comparison among some recent criteria, *Theor. Appl. Fract. Mech.*, 85 (2016) 217-226. DOI:10.1016/j.tafmec.2016.02.001.
- [26] Yosibash, Z., Bussiba, A., Gilad, I., Failure criteria for brittle elastic materials, *Int. J. Fract.*, 125 (2004) 307–333. DOI: 10.1023/B:FRAC.0000022244.31825.3b.
- [27] Qian, J., Hasebe, N., Property of eigenvalues and eigenfunctions for an interface V-notch in antiplane elasticity, *Eng. Fract. Mech.*, 56 (1997) 729–734. DOI: 10.1016/S0013-7944(97)00004-0.
- [28] Gough, H.J., Pollard, H. V., Properties of some materials for cast crankshafts, with special reference to combined stresses, *Arch. Proc. Inst. Automob. Eng.*, 31 (1936) 821–893. DOI: 10.1243/PIAE_PROC_1936_031_040_02.
- [29] Lazzarin, P., Sonsino, C.M., Zambardi, R., A notch stress intensity approach to assess the multiaxial fatigue strength of welded tube-to-flange joints subjected to combined loadings, *Fatigue Fract. Eng. Mater. Struct.*, 27 (2004) 127–140. DOI: 10.1111/j.1460-2695.2004.00733.x.
- [30] Gallo, P., Berto, F., Glinka, G Generalized approach to estimation of strains and stresses at blunt V-notches under non-localized creep, *Fatigue Fract. Eng. Mater. Struct.*, 39 (2016) 292-306.